

Real-Scale Investigation of the Washboard Phenomenon on Unpaved Roads

Laura Ibagón, Juan P. Villacreses

College of Science and Engineering, Universidad San Francisco de Quito, Quito, Ecuador.

Bernardo Caicedo

Department of Civil and Environmental Engineering, Universidad de los Andes, Bogotá Colombia,
bcaicedo@uniandes.edu.co

ABSTRACT: Washboard, or road corrugation, commonly forms on unpaved roads as a result of the continuous passage of vehicles. These surface deformations not only affect the driver comfort and safety, but also influence vehicle performance and road lifespan. Although this phenomenon is widely observed, it remains scarcely studied. This research makes an effort to explore this gap through a detailed analysis of the geotechnical characteristics of the road materials, complemented by traffic count surveys and drone-based surface mapping to evaluate road morphology. Furthermore, a real-scale experimental setup using a pickup truck is proposed to examine vehicle responses when traveling at various speeds over an unpaved road section. The results provide some insights into the mechanisms driving washboard formation, while also highlighting unresolved aspects that require further research.

KEYWORDS: Washboard effect, soil wheel interaction, corrugation, critical velocity, soil undulations, unpaved roads.

1 INTRODUCTION

Washboard, also known as corrugations, are surface ripples (Figure. 1) that appear on unpaved roads, creating discomfort for drivers and affecting vehicle performance. Research on this phenomenon began in 1938 and has been developed through theoretical studies, laboratory experiments, and field observations aimed at understanding how these patterns form.

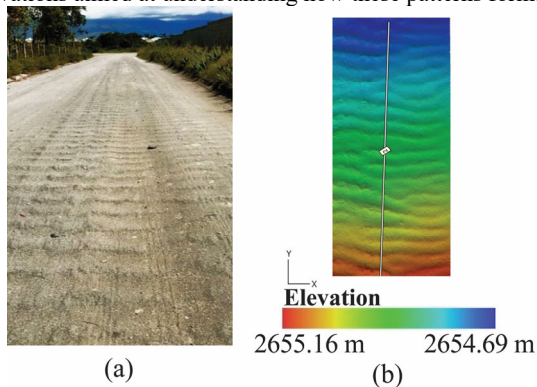


Figure 1. Washboard on unpaved roads in Pichincha, Ecuador.

Relton (1938) described this phenomenon as a “relaxation oscillation” caused by stick-slip dynamics. He suggested that the wheel pushing material ahead of it, is what creates the ripples. Mather (1963) built on this work developed the first experimental model based on field observations. Using a wheel rolling over granular surfaces of different particle sizes and shapes, he found that velocity plays a key role in the formation of corrugations. Riley and Furry (1973) later introduced a combined theoretical and experimental model of a road–vehicle system, represented as a mass-spring-damper setup. Their results, supported by laboratory experiments, showed that vehicle speed, weight, and tire pressure all influence the development of surface undulations.

In 2006, Shoop et al., (2006) conducted detailed field observations of seasonal deterioration on unpaved roads, showing that washboard can form during wet spring conditions due to thawing, not just in dry seasons.

Taberlet et al. (2007) expanded this understanding by comparing laboratory tests with soft-particle numerical simulations and proposed an expression to estimate the wheel’s normal force. Bitbol et al. (2009) highlighted velocity as a critical parameter and defined a threshold velocity using dimensionless analysis. Hewitt et al. (2011) showed that

corrugation can appear even after just one plow pass at a critical velocity.

In 2011, Mahgoub et al., proposed a predictive model based on data from 16 gravel roads, using factors like aggregate gradation, angularity, moisture content, subgrade density, depth to densified subgrade, and average vehicle speed. Their results showed that larger volumes of disturbed material lead to more severe corrugations. In 2021, Abu Daoud and Ksaibati investigated road geometry on corrugation severity. In 2022, Abu Daoud et la., analyzed more than 4000 road surface images and used deep learning to automatically classify corrugation patterns, reducing the need for manual inspections.

More recently, Caicedo and Aguetant (2022) proposed an experimental set up capable of evaluating surface corrugations. This work assessed soil undulations and dynamic forces under variable wheel velocities. This experimental device was also employed by Ibagón et al., (2023), to perform controlled tests to identify the main factors influencing washboard development on unpaved roads. Then, Ibagón et al., (2025) (a) proposed a stress-oriented theoretical model that replicates the patterns observed in the experiments. Finally, Ibagón et al., (2025) (b), evaluated geocell reinforcement as a mechanism to mitigate corrugation.

This study is organized as follows: The first section introduces the washboard phenomenon and previous research approaches. The second section describes the experimental device and unpaved road features. The third section presents the results, and the final section discusses the findings, addressing both current knowledge and remaining open questions.

2 METHODOLOGY

2.1 Road Material Characterization

An unpaved road with washboard phenomenon was selected for this study in Pichincha, Ecuador, as illustrated in Figure 2. Soil samples were collected from the road and particle size distribution, dry density, shear wave velocity, vehicle counts and drone surveying were assessed.

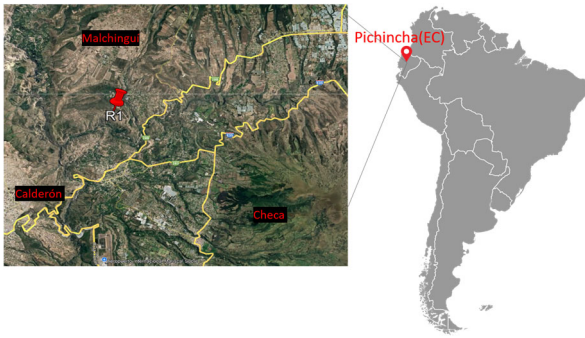


Figure 2. Unpaved road R1 in Pichincha, Ecuador.

The soil sample collected from the location was classified as poorly graded sand (SP), with median grain sizes (d_{50}) of 0.30 mm. Particle size distribution tests were performed according to ASTM D6913 and the results are presented in Figure 3.

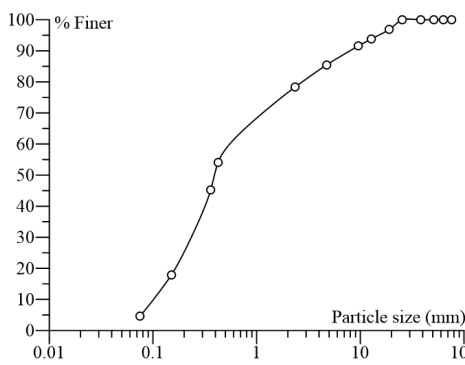


Figure 3. Particle Size Distribution of soil sample from road R1

Additionally, Modified Proctor tests were performed on each soil sample following the procedure in D1557, as illustrated in Figure. 4. The result showed a maximum high density of 1.81 g/cm³, with an optimal water content close to 11%. Likewise, in-situ measurements of water content and soil density were conducted. As a result, a dry density of 1.84 g/cm³ and a water content of 8.38% were registered. This result determined that the field density exceeded the maximum by 2%, and indicate that the road achieved a dense condition as a result of compaction during construction.

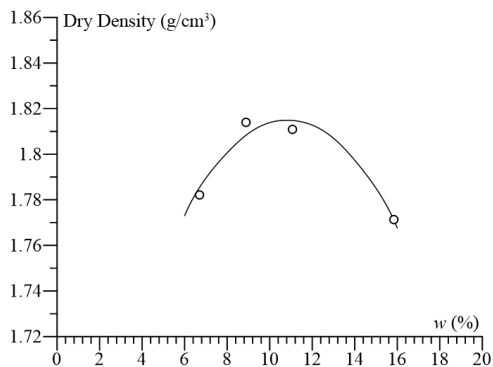


Figure 4. Modified Proctor test

Road material characterization also included Multichannel Analysis of Surface Waves (MASW) geophysical testing. This technique estimates the variation of shear wave velocity (V_s) with depth and is widely applied in geotechnical engineering for near-surface characterization (Socco and Strobbia, 2004).

MASW is employed in the field due to the simplicity of wave generation, detection, and data processing. It relies on the propagation of surface waves, primarily Rayleigh waves, whose velocities vary with frequency and subsurface conditions. In this study, a hammer was used as an active seismic source, and multiple geophones were deployed to record the dispersion of the surface waves (Ahmed JR Al-Heety et al., 2021). The experimental setup is shown in Figure. 5a and 5b. The test was carried out to obtain one-dimensional (1D) shear (S) wave profiles.

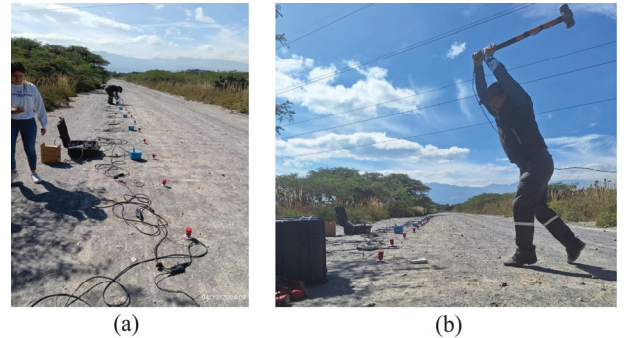


Figure 5. MASW geophysical tests. (a) Geophones placed to record surface wave dispersion, (b) Active seismic source applied through a hammer

A seismic array consisting of vertically oriented geophones was installed along a 20 m line with uniform spacing. In addition, seven three-component geophones were deployed to record multidirectional seismic wave propagation. Data acquisition was performed using a Geometrics Geode digitizer. A 20 kg sledgehammer served as the seismic source, striking a metallic plate positioned at every second geophone along the array. To reduce random seismic noise from sources such as footsteps, wind, and passing vehicles, five impacts were recorded at each location, and the resulting signals were combined to enhance the signal-to-noise ratio.

This procedure aimed to characterize the subsurface by determining shear wave velocity (V_s). MASW results showed V_s values of approximately 150 m/s, corresponding to the upper 40 cm of depth.

2.2 Road Surveying

Road corrugation was evaluated on an unpaved road in Pichincha, Ecuador, using an uncrewed aerial vehicle (UAV), as illustrated in Figure. 6(a, b). This method offers a practical and accessible methodology of accurately capturing road profiles. For the surveys, DJI Mini 2SE and DJI Mini 3 drones were deployed, with flight altitudes between 0.5 m and 2 m determined from preliminary field tests.

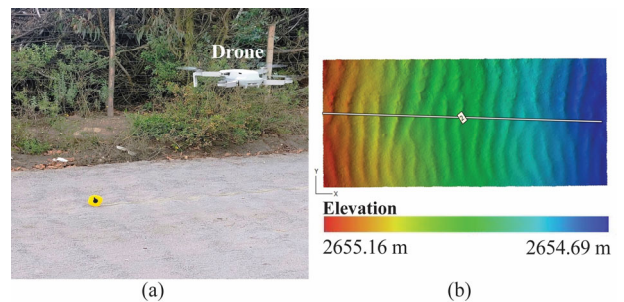


Figure 6. Drone surveying methodology.

Figure 7 presents the results for the corrugated road, with surface profiles analyzed over a 1.6 m length. The road exhibited a mean peak to peak wave amplitude of 20.6 mm.

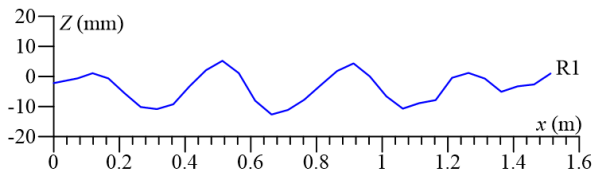


Figure 7. Road profile measured with drone surveying.

Traffic counts and speed measurements were conducted for a sample of 40 vehicles traveling on the evaluated roads. The road registered a median of approximately 31 km/h, with values ranging from 28 km/h to 34 km/h.

2.3 Measurement device

For this study, the experimental setup consisted of a pickup truck, with a laser sensor and two accelerometers, all installed at the rear of the vehicle as shown in Figure 8. The laser sensor, used to record the road profile and identify corrugations, was installed on an external steel frame secured to the rear bumper (Figure. 8b). This frame also held one accelerometer, aligned vertically with the laser sensor to measure cargo bed motion as the vehicle crossed the corrugated surface. A second accelerometer was attached to the rear axle to capture wheel movement on the unpaved road (Figure. 8a). Data were acquired using a wired NI 9222 system at a sampling rate of 10,240 Hz (Figure. 8c). Tests involved single vehicle passes at constant speeds between 10 and 60 km/h on the road.

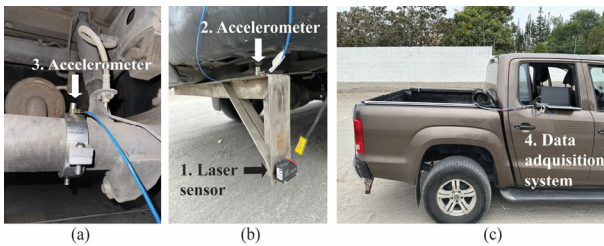


Figure 8. Experimental set-up used for real road measurements. (a) Rear axle accelerometer, (b) Cargo bed accelerometer and laser sensor, (c) Data acquisition system.

3 RESULTS

Figure 9 and 10 illustrates the vertical accelerations measured at the cargo bed (a_1) and rear axle (a_2) for vehicle speeds of 10, 20, 40, and 60 km/h on the evaluated road. These raw data highlight how the vehicle's dynamic response changes with velocity.

For this road, at lower speeds (10 and 20 km/h), accelerations at the cargo bed exceeded those at the rear axle. At 10 km/h, maximum accelerations of 1.31 m/s^2 were registered for the cargo bed and 1.04 m/s^2 for the rear axle, representing an approximate 26% amplification. A similar pattern occurred at 20 km/h, with 4.19 m/s^2 and 2.91 m/s^2 , for the cargo bed and the rear axle respectively, which corresponds to a 44% amplification, possibly due to vibration transmission through the vehicle structure.

At higher speeds, the trend reversed. At 40 km/h, the cargo bed recorded 6.93 m/s^2 compared to 14.17 m/s^2 at the rear axle, a 51% reduction possible due to the suspension filtering. At 60 km/h, accelerations were 9.44 m/s^2 for the cargo bed and 13.20 m/s^2 for the rear axle, indicating a 28% reduction. While suspension damping remained effective at this speed, its efficiency was lower than at 40 km/h.

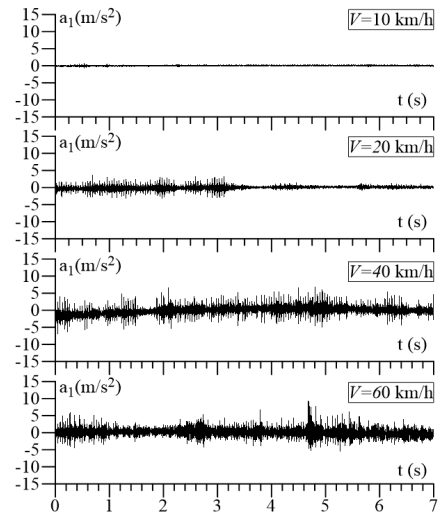


Figure 9. Vehicle accelerations for R1 and varying velocities. Cargo bed accelerations (a_1) in the time domain.

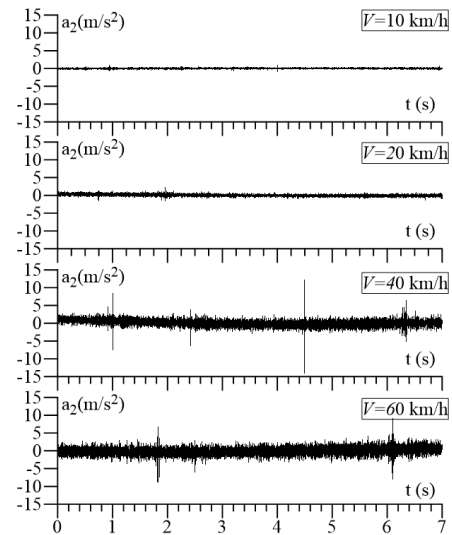


Figure 10. Vehicle accelerations for R1 and varying velocities. Rear axle accelerations (a_2) in the time domain.

4 CONCLUSIONS

This study integrated geotechnical testing, MASW measurements, drone-based surface surveying, traffic monitoring, and full-scale vehicle instrumentation to characterize washboard behavior on unpaved roads in Pichincha, Ecuador. The road material was found to be a dense, well-compacted sandy soil, with near-surface stiffness consistent with shear-wave velocities on the order of 150 m/s in the upper 0.4 m. Drone surveys were employed to quantify corrugation geometry, yielding representative mean undulation amplitudes on the order of twenty mm. Traffic counts indicated typical operating speeds near 30–40 km/h, a range that aligns with velocity-dependent changes in the measured dynamic response.

Full-scale measurements revealed a clear speed dependence: at lower speeds (≈ 10 – 20 km/h), cargo-bed accelerations were amplified relative to those at the rear axle, whereas at higher speeds (≈ 40 – 60 km/h) the suspension attenuated cargo-bed peaks relative to axle input, with the most effective filtering observed around 40 km/h. Taken together,

these results underscore the coupling among surface geometry, material state, and vehicle speed in governing the onset and manifestation of corrugations.

Future work needs to be conducted to develop a deeper understanding of suspension behavior to better assess vehicle performance on unpaved roads. Monitoring should also be extended in time to capture seasonal moisture effects. Finally, mitigation strategies, such as surface reinforcement and speed management, needs to be evaluated to reduce corrugation growth and its impact on safety, comfort, and maintenance.

5 REFERENCES

- Ahmed JR Al-Heety, Mohammed Hassouneh, and Fathi M Abdullah. Application of masw and ert methods for geotechnical site characterization: A case study for roads construction and infrastructure assessment in abu dhabi, uae. *Journal of Applied Geophysics*, 193:104408, 2021.
- ASTM D1557: Standard Test Methods for Laboratory Compaction Characteristics of Soil Using Modified Effort (56,000 ft-lbf/ft³ (2,700 kN-m/m³)), 2021. URL <https://www.astm.org/d1557-12r21.html>. Developed by Subcommittee: D18.03, Last Updated: Jul 05, 2021.
- ASTM. D6913: Standard test methods for particle-size distribution (gradation) of soils using sieve analysis. ASTM International, D6913, 2017.
- Bitbol, A.-F., Taberlet, N., Morris, S. W., and McElwaine, J. N. (2009). Scaling and dynamics of washboard roads. Ph.D. thesis, Cambridge University.
- Caicedo, B., & Aguetant, G. (2022). Physical Modeling of the Washboard Effect on Unpaved Roads. In *Advances in Transportation Geotechnics IV* (pp. 243-251). Springer, Cham.
- Hewitt, I., Balmfort, N. J., and McElwaine, J. N. (2011). Granular and fluid washboard. PhD thesis, Cambridge University
- Ibagón, L., Caicedo, B., Villacreses, J. P., & Yépez, F. (2023). Modelling of washboard effect on unpaved roads experimental evidence on non-cohesive materials. *Transportation Geotechnics*, 41, 101015.
- Ibagón, L., Caicedo, B., Villacreses, J. P., & Achury-Florian, Á. (2025). Theoretical modelling of the washboard phenomenon on unpaved roads. *Transportation Geotechnics*, 101484.
- Ibagón, L., Caicedo, B., Villacreses, J. P., & López-Caballero, F. (2025). Mitigating washboard effect: A study on geocells as soil reinforcement for unpaved roads. *Geotextiles and Geomembranes*, 53(6), 1433-1445.
- J. G. Riley and Furry, R. B. (1973). Simulation of the road-corrugation phenomenon *Highway Research Record*, 438, 54.
- K. B. Mather, *Civ. Eng. Pub. Works Rev.*, 57, 617 (1963), and *Civ. Eng. Pub. Works Rev.*, 57, 781 (1963).
- Mahgoub, H., Bennett, C., & Selim, A. (2011). Analysis of factors causing corrugation of gravel roads. *Transportation research record*, 2204(1), 3-10.
- Osama Abu Daoud and Khaled Ksaibati. Studying the effect of gravel roads geometric features on corrugation behavior. *International Journal of Pavement Research and Technology*, pages 1–9, 2021.
- Relton, F. E. (1938). Corrugations on roads. *Roads and Road Construction*, 16(190), 340-342.
- Shoop, S., Haehnel, R., Janoo, V., Harjes, D., & Liston, R. (2006). Seasonal deterioration of unsurfaced roads. *Journal of geotechnical and geoenvironmental engineering*, 132(7), 852-860.
- Taberlet, N., Morris, S. W., & McElwaine, J. N. (2007). Washboard road: the dynamics of granular ripples formed by rolling wheels. *Physical review letters*, 99(6), 068003.